ACS APPLIED MATERIALS & INTERFACES

Letter

www.acsami.org

Tailoring Indium Oxide Nanocrystal Synthesis Conditions for Air-Stable High-Performance Solution-Processed Thin-Film Transistors

Sarah L. Swisher,* Steven K. Volkman, and Vivek Subramanian*

Department of Electrical Engineering and Computer Sciences, University of California, Berkeley, California, United States

Supporting Information

ABSTRACT: Semiconducting metal oxides (ZnO, SnO_2, In_2O_3, and combinations thereof) are a uniquely interesting family of materials because of their high carrier mobilities in the amorphous and generally disordered states, and solution-processed routes to these materials are of particular interest to the printed electronics community. Colloidal nanocrystal routes to these materials are particularly interesting, because nanocrystals may be formulated with tunable surface properties into stable inks, and printed to form devices in an additive manner. We report our investigation of an In_2O_3 nanocrystal synthesis for high-performance solution-deposited semiconductor layers for thin-film transistors (TFTs). We studied the effects of various synthesis parameters on the nanocrystals themselves, and how those changes ultimately impacted the performance of TFTs. Using a sintered film of solution-deposited In_2O_3 nanocrystals as the TFT channel material, we fabricated devices that exhibit field effect mobility of 10 $cm^2/(V\ s)$ and an on/off current ratio greater than 1×10^6. These results outperform previous air-stable nanocrystal TFTs, and demonstrate the suitability of colloidal nanocrystal inks for high-performance printed electronics.

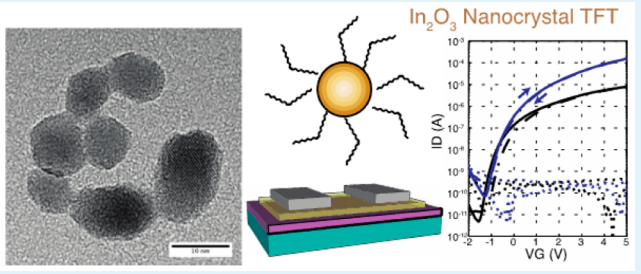

KEYWORDS: *indium oxide, In_2O_3, nanocrystal synthesis, thin-film transistor, nanocrystal transistor, printed electronics, solution processing*

Flexible electronic systems have attracted significant interest in recent years as a pathway to applications that benefit from large-area form factors and mechanical flexibility. Advances in thin-film materials and devices over the past decades have helped to drive the development of flexible electronic systems such as flexible displays, RFID tags, electronic textiles, bioinspired sensors, and wearable or implantable medical devices.[1−4] Printing solution-based electronic materials is a particularly desirable path toward flexible electronics because it is an additive process, which reduces material usage and process complexity while enabling the integration of different functional materials on an inexpensive substrate.[4,5]

From a materials perspective, printed electronics require highly repeatable synthetic methods to produce consistently high-quality inks. Although most work on printed electronics has focused on organic systems, inorganic materials are particularly interesting in this regard because they offer potential advantages in terms of performance, environmental stability, and transparency. Two key pathways toward solution-processed inorganic semiconductor materials have been recently explored for TFTs: (1) sol−gels using metal precursor solutions, and (2) colloidal nanocrystals. Despite the reports of high-performance sol−gel TFTs, it is widely recognized within the community that the device performance can be very sensitive to precursor solution preparation and processing (i.e., the sit-time or "aging" of the precursor solution, and how quickly the film is dried or annealed after deposition). For example, Lee et al. recently demonstrated that controlling the temperature of the precursor solution alters the ionic species in solution; this changes the metal-oxide lattice formation in the annealed film, thus significantly impacting the transport in the TFT.[6] Similarly, we have found that although sol−gels can indeed provide high-performance semiconductors,[7] in some cases, the device performance is degraded as the sol−gel ink ages (see the Supporting Information). Unfortunately, the myriad process sensitivities have not been thoroughly studied, and their impacts are not always understood. These instabilities pose challenges both in terms of device uniformity and, ultimately, the large-scale manufacturability of such an approach to printed electronics.

Though much of the current printed electronics literature focuses on ink formulations based on inorganic sol−gels,[7−14] colloidal semiconductor nanocrystals are an attractive alternative that may provide more stable inks. Colloidal nanocrystals can be easily solubilized in printable solvents, providing a highly crystalline and phase-pure material in solution. The ligands that help control particle growth during nanocrystal synthesis and provide solubility in the final ink formulation can be tuned to favor outcomes such as high mass loading or low sintering

Received: January 30, 2015
Accepted: April 27, 2015
Published: April 27, 2015

ACS Publications © 2015 American Chemical Society

DOI: 10.1021/acsami.5b00893
ACS Appl. Mater. Interfaces 2015, 7, 10069−10075

Scheme 1. Indium Oxide Nanocrystal Reaction

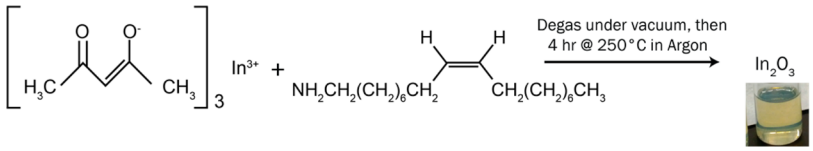

temperature,[15] and postsynthesis ligand exchange procedures can allow further tailoring of the nanocrystal surface properties.[16] Unlike sol–gel formulations, the size and shape of colloidal nanocrystals can be adjusted during synthesis, and are thus unaffected by the thermal budget constraints of the substrate. In fact, this control over morphology and surface chemistry has already led to the widespread use of sintered metal nanoparticles to form electrodes and interconnects in printed electronics.

Colloidal nanocrystals for thin-film semiconductors have been explored as well, though that body of work has primarily focused on exploiting the high degree of electronic coupling that is achieved in quantum confined particles of metal chalcogenides (CdSe, CdTe, PbSe, etc.); Talapin et al. provide a thorough review.[17] The significant drawbacks of these materials have so far outweighed their potential benefits, however; they typically deliver poor TFT mobility due to the degraded transport resulting from the ligands that maintain quantum confinement in the film, they are inherently toxic, and their extreme sensitivity to air and moisture requires all device fabrication and electrical characterization to be performed in an inert-atmosphere glovebox. The recent development of inorganic ligands[16] and encapsulation schemes using atomic layer deposition (ALD) prior to air exposure[18] have led to dramatic improvements in the electron transport of these quantum dot films. Within the past year, Law and co-workers reported a record air-stable field-effect mobility of ∼7 $cm^2/(V\ s)$ in a quantum dot transistor.[18] Although these advancements are promising, the inherent toxicity and air sensitivity of metal chalcogenide quantum dots pose significant technological hurdles to their use in large-scale printing applications.

Recently, solution-processable routes to post-transition metal oxides (ZnO, SnO_2, In_2O_3, and combinations thereof) have been an area of intense focus among the printed electronics research community[7−14] because this family of materials can deliver electron mobilities in the amorphous phase an order of magnitude higher than amorphous silicon.[19] Many of these materials are also nontoxic, adding to their appeal. In these systems, indium is thought to be a key component for obtaining good transport properties,[20] and is included in many ternary and quaternary metal oxide semiconductors (IZO, IGZO, IZTO, etc.).[8−14,19] Pure indium oxide has been less thoroughly studied as a solution-processed semiconductor material, though several reports of sol–gel indium oxide transistors thus far have been extremely promising.[10−12] Indium oxide nanocrystals are particularly attractive for solution-processed semiconductor thin films because they may be able to combine the high performance and straightforward processing techniques of sol–gels with the crystalline purity and size control of colloidal nanocrystals. Several groups have reported on the synthesis of In_2O_3 nanocrystals,[21−24] but the few reports of indium oxide nanoparticle TFTs have exhibited poor transport (mobility values of 0.004–0.8 $cm^2/(V\ s)$) and poor electrostatic control (on/off current ratios of $\sim 1 \times 10^3$ and lower).[25,26] Further, the effect of synthetic conditions—including choice of reagents, reaction temperature, and purification methods—on the performance of printed electronics has not yet been studied. In this work, we realize a dramatic improvement in performance in indium oxide nanocrystal TFTs; we show how nanoparticle synthetic and device processing conditions can be optimized to demonstrate high-performance transistors using colloidal In_2O_3 nanocrystals as the solution-processed channel material, without the need for specialized inert-atmosphere fabrication or testing procedures. The motivation to use nanocrystals in this case is not to exploit quantum confinement effects; instead, we employ a sintering technique that deliberately removes encapsulation molecules and excess solvent, converting the solution-deposited layer into a high-performance thin film.[27,28] Furthermore, we investigate the impact of a vacuum degassing step and reaction temperature during the synthesis of indium oxide nanocrystals on their performance as the semiconducting layer in TFTs. We report a synthetic method that yields a high-quality indium oxide nanocrystal ink for high-performance solution-processed electronics, delivering transistors with performance characteristics better than previously reported indium oxide nanoparticles[25,26] or air-stable quantum dots,[18] and comparable to most sol–gel systems[9,13,14] while delivering a pathway to stable ink formulation.

We start from a method for obtaining highly crystalline colloidal In_2O_3 nanocrystals published by Seo et al.[21] We synthesized soluble indium oxide nanocrystals utilizing a one-pot thermal decomposition synthesis performed underan argon atmosphere using standard air-free Schlenk line techniques (Scheme 1). In a typical procedure, 1 mmol of indium(III) acetylacetonate was mixed with 40 mmol of oleylamine in a round-bottom-flask. The reaction was placed under vacuum (∼100 mTorr), heated to 70 °C over 10 min, then held at that temperature for 30 min to degas. The reaction was flushed three times with argon during the degassing period. The solution was then heated to 250 °C over 30 min under flowing argon, and the reaction was allowed to proceed at that temperature for 4 h. After cooling to room temperature, the flask was opened to air. Insoluble reaction products (if any) were removed by centrifugation, and then the nanocrystals were precipitated by centrifugation and washed with ethanol. The nanocrystals were redispersed in chloroform at a concentration of approximately 1 wt % and transferred to a glass vial for storage.

The size and morphology of the nanocrystals were investigated using transmission electron microscopy (TEM), and crystal structure was determined using X-ray diffraction. Bottom-gate, top-contact thin-film transistor (TFT) structures were fabricated utilizing the indium oxide nanocrystal solution as the channel material. For convenience and repeatability of testing, heavily doped silicon wafers with 100 nm thermally grown SiO_2 were used as the gate electrode and gate oxide, respectively. It is generally observed that high-k dielectrics deliver devices with higher performance when used as gate dielectrics for metal oxide semiconductor channels. Therefore,

DOI: 10.1021/acsami.5b00893
ACS Appl. Mater. Interfaces 2015, 7, 10069−10075

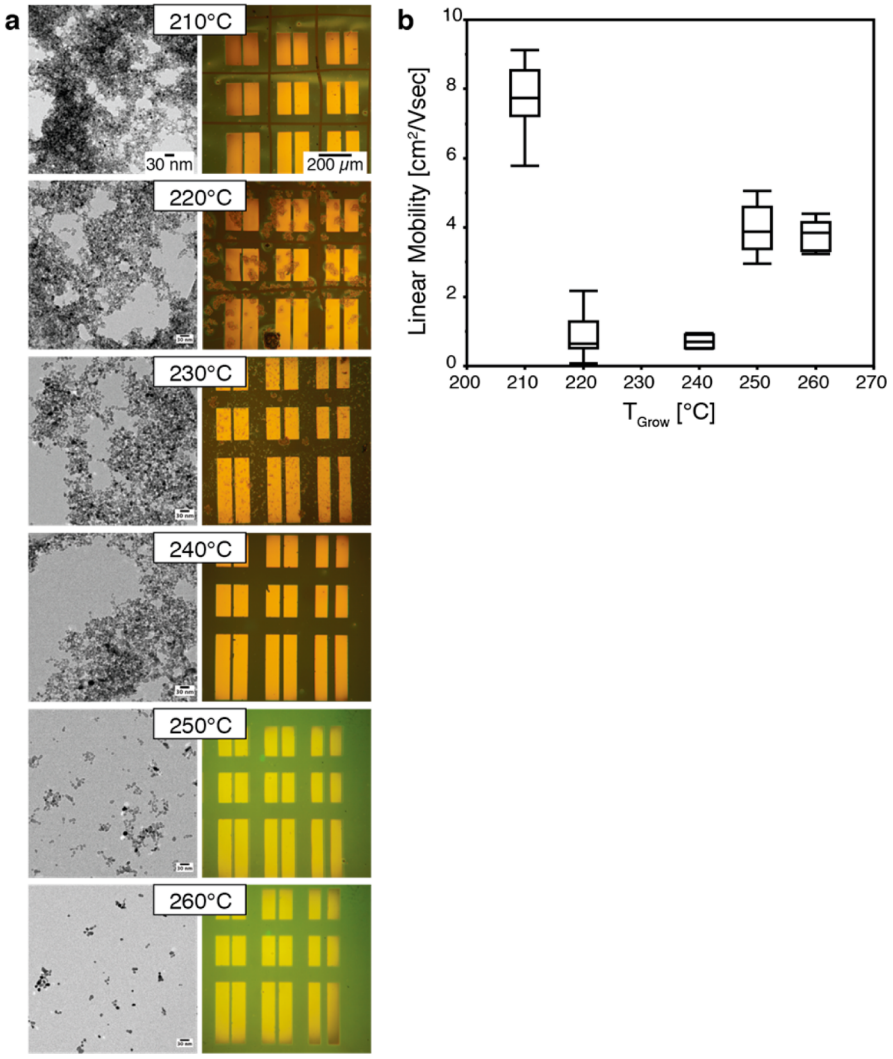

Figure 1. Effects of growth temperature during synthesis (T_{Grow}) on nanocrystal solubility, film quality, and TFT performance. (a) TEM images of nanocrystals synthesized at temperatures from 210—260 °C, and optical microscope images of the corresponding TFT samples. Scale bar = 30 nm for TEM images; scale bar = 200 μm for optical micrographs. (b) Linear field-effect mobility from TFTs fabricated with nanocrystals from each synthesis temperature. Mobility could not be extracted for devices from the T_{Grow} = 230 °C sample because the film was not continuous, and no working devices could be fabricated.

high-performance devices were also fabricated using 40 nm of ZrO_2 deposited by atomic layer deposition (ALD) as the gate dielectric instead of SiO_2; all other processing was identical. Indium oxide nanocrystals were spin-coated onto the gate oxide, followed by an oxygen anneal for 1 h at 500 °C. Film morphology and surface roughness were measured by atomic force microscopy (AFM). Finally, aluminum source/drain electrodes (50 nm) were deposited by thermal evaporation through a shadow mask to produce TFTs. With the exception of the oxygen anneal, all processing was performed in air.

Many studies have demonstrated that the presence of even a small amount of water or organic impurities in a nanocrystal synthesis can have a significant impact on the outcome of the reaction.[29] Thus, we investigated the effect of a vacuum degassing step in the In_2O_3 nanocrystal synthesis procedure. We compared the In_2O_3 particles resulting from a synthesis that included a 30 min degas step at 70 °C, during which time the reaction was purged three times with high-purity argon (our standard reaction) with an otherwise identical reaction with the degas step omitted. We observed a dramatic improvement in the solubility of the final product in the reaction that included the degas step. When the two samples were redispersed in chloroform after collection from the reaction and washing in ethanol, the sample that underwent the vacuum degassing step dissolved immediately into a nearly transparent yellowish-blue solution. In contrast, upon dissolving the sample that was simply ramped to the growth temperature under argon flow without the vacuum step, we obtained a cloudy yellow solution. The marked improvement in solubility and lack of aggregation in solution was also observed by TEM (see the Supporting Information).

In addition to the removal of water, the improvement in the solubility evident from this experiment may also be partially attributed to the removal of other contaminants present in the oleylamine. Technical-grade oleylamine is only 70% pure as purchased, though it contains >98% primary amines. Shorter-chain primary amines and saturated primary alkylamines will generally have lower boiling points than the oleylamine and thus be more easily removed during the vacuum degas step; this purification step may have contributed to the high batch-to-batch consistency we observed following the synthetic procedure outline above. For example, despite the similar

DOI: 10.1021/acsami.5b00893
ACS Appl. Mater. Interfaces 2015, 7, 10069−10075

length and basicity of oleylamine and octadecylamine, previous studies have shown that using oleylamine as the stabilizer allowed better control of nanoparticle size.[30] In a study of Au nanoparticles, Lu and co-workers attributed a more stable precursor complex to the formation of a coordination bond between the C═C in oleylamine and the Au precursor, thus decreasing the precursor decomposition rate and the nanoparticle growth rate.

Nanocrystal growth temperature is one of the most critical aspects of the synthetic procedure.[29] Providing sufficient heat to the reaction turns the precursors into active atomic or molecular species (monomers). The characteristics of the nanoparticles are determined by the competing processes of nucleation and growth during the reaction. In the nucleation phase, precursors rapidly decompose resulting in a supersaturation of monomers, then the nucleation of nanocrystal "seeds". Monomers remaining in solution following the nucleation event are consumed during the growth phase: monomers add to the nanocrystal seeds in solution, and the particles grow. To obtain high-quality crystals, the reaction temperature must be sufficiently high to allow rearrangement of the atoms during growth, and to provide dynamic solvation by the surfactant molecules.[29] The binding strength of surfactant molecules and the stability and diffusion rate of the intermediate complexes in the reaction solution are all strongly dependent on the reaction temperature: increasing the temperature greatly reduces the stability of intermediate complexes in the solution and increases their diffusion rates, thus inducing nanocrystal nucleation and growth.[29] Excessive temperature, however, can lead to rapid and uncontrolled growth, such that subtle kinetic or energetic effects cannot be leveraged to precisely control particle size and shape. During the course of the In_2O_3 synthesis, we observed a visible change in the reaction from transparent yellow to dark gray at a temperature of approximately 215 °C, and then another abrupt change back to a yellowish translucent color at approximately 240 °C. No further color change was observed up to 260 °C, until the reaction was cooled to room temperature. To investigate the effect of nanocrystal growth temperature on the performance of solution-processed nanocrystal TFTs, we repeated the synthesis with varied reaction temperatures between 210 and 260 °C. We examined each batch of nanocrystals using TEM, then fabricated transistors and used the extracted linear field-effect mobility as a metric for comparing TFT performance.

At low growth temperatures, we observed polydisperse nanocrystals with poor solubility, resulting in nonuniform solution-processed semiconductor films. Large multicrystalline particles were observed in the TEM images for temperatures up to 230 °C (Figure 1a, left). It is unclear from the TEM images whether the large particles are the result of a small number of nucleation events followed by excessive growth, or if they are aggregations of many smaller particles. These nanocrystal solutions appeared cloudy immediately following synthesis, and after ∼24 h, the particles had flocculated and precipitated out of solution. Correspondingly, spin-coated films made using these poorly solubilized particles were nonuniform at the device scale, exhibiting thick streaks and/or patchy deposition (Figure 1a, right). For growth temperatures below 230 °C, the particles in the ink appeared large enough to form thick films that contain percolation networks between the source and drain electrodes. At a growth temperature of 230 °C, the semiconductor film appeared patchy and discontinuous; as a result, no TFTs could be fabricated.

As the growth temperature increased, there were fewer large multicrystalline particles observed in TEM. This is consistent with increased nucleation: a larger number of particle "seeds" form, and growth is limited by the low concentration of monomers in the reaction solution. The nanocrystals were more uniform in size and their solubility improved; as a result, the films became smoother and more continuous. At 240 °C, many large particles were still present; by 250 °C, the particles were relatively uniform in size and well-dispersed. At these temperatures, uniformly smooth films were observed at the device scale using optical microscopy. We further characterized the nanoscale film morphology using atomic force microscopy (AFM) for spin-coated films of In_2O_3 nanocrystals grown at 250 °C and observed a ∼32 nm thick film with surface roughness of 4 nm_{RMS} (see the Supporting Information).

Achieving such thin, smooth semiconductor films is critical to maximize TFT performance, and to minimize variation between devices on large-area substrates. Interestingly, the TFT mobility does not vary monotonically with nanocrystal growth temperature (Figure 1b). At lower growth temperatures, the indium oxide nanocrystal synthesis appears to be growth-dominated, so the solution consists of large multicrystalline nanoparticles. Increasing the growth temperature results in a larger number of smaller nanocrystals; this improves solubility and produces thin films that are smoother and more compact. Thus, we hypothesize that as the nanocrystal growth temperature increases, the TFT mobility first drops as the crystallite size shrinks, then it increases as the channel becomes denser and more continuous. In addition, the high mobility of the 210 °C sample could be partially attributed to an incomplete precursor-to-monomer reaction, producing a mixture of nanocrystals and intermediate precursor complexes. In this case, nanocrystals would essentially be deposited in a sol−gel, accounting for the higher mobility. This hypothesis also explains the instability of the low-growth-temperature inks, because sol−gels often rapidly form precipitates. It is also consistent with the fact that the reaction is run below or near the temperature where a color change is observed (215 °C), which most likely indicates the monomer formation or a nucleation event. Because all devices underwent a postdeposition anneal at 500 °C for 1 h, residual ligands in the film are not likely to be a dominant factor in the mobility variation.

The best combination of film morphology and TFT mobility is achieved with a nanocrystal growth temperature of 250 °C. No further improvements in solubility or TFT performance were observed by raising the growth temperature above 250 °C. Though the highest mobility was actually achieved using particles grown at only 210 °C, it is important to note that this result is ultimately undesirable for printed electronics because of the poor ink stability and film uniformity. Aggregation of the nanocrystals in the ink would prohibit its use in inkjet and gravure printing applications because of nozzle clogging and uncontrollable printing due to changing fluid properties. Film quality is particularly problematic in fully printed devices, because the deleterious effects of film roughness are compounded as additional layers are deposited.

Having determined that 250 °C was the optimal nanocrystal growth temperature for our TFTs, we further characterized the as-synthesized material under this synthetic condition. A bright-field TEM image of the indium oxide nanocrystals obtained from a standard synthesis showed roughly spheroidal particles

DOI: 10.1021/acsami.5b00893
ACS Appl. Mater. Interfaces 2015, 7, 10069−10075

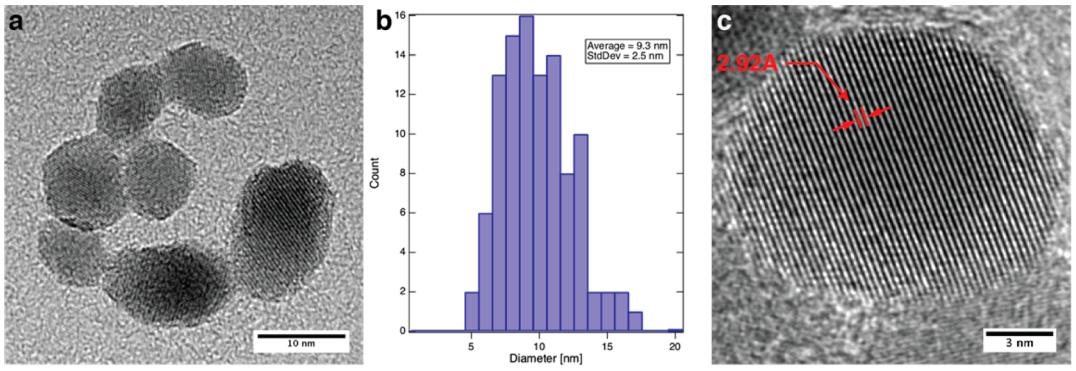

Figure 2. (a) Transmission electron micrograph (TEM) of In_2O_3 nanocrystals from the air-free reaction of indium(III) acetylacetonate and oleylamine at 250 °C. Scale bar = 10 nm. (b) Histogram of nanocrystal diameter calculated from >100 individual particles. (c) High-resolution TEM confirming the single-crystalline nature of the particles; fringe spacing of 2.92 Å corresponds to the d_{222} interplanar spacing of bulk cubic In_2O_3. Scale bar = 3 nm.

(Figure 2a) that are easily dispersed in nonpolar organic solvents. Statistics collected from >100 individual particles indicate that the average diameter of the as-prepared particles is 9.3 nm ±2.5 nm (Figure 2b). High-resolution TEM (Figure 2c) confirmed the single-crystalline nature of the particles as prepared; we measured 2.92 Å spacing between lattice fringes in the phase-contrast image, corresponding to the (222) interplanar spacing of bulk cubic In_2O_3 (PDF no. 00−006−0416).

The X-ray diffraction (XRD) pattern shown in Figure 3 for the nanocrystals as-deposited (dried in air at room temperature) is well matched to that of bulk cubic In_2O_3 (PDF no. 00−006−0416). The average crystallite size calculated from the Scherrer equation using the full-width at half-maximum (fwhm) of the most intense reflection peak (2θ = 30.5°) is 10 nm. The agreement of the particle size from TEM and the crystallite size from XRD further confirms the single-crystalline nature of the In_2O_3 nanocrystals produced using this synthetic procedure, suggesting that a reaction temperature of 250 °C is sufficiently high to allow rearrangement of atoms during nanocrystal growth.

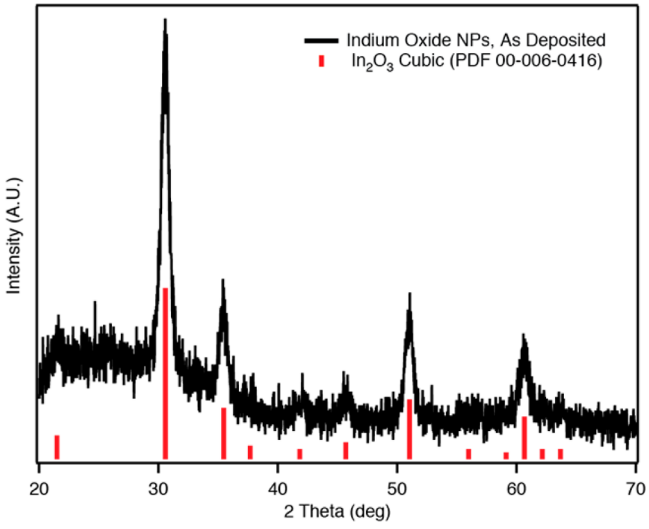

Figure 3. X-ray diffraction pattern of indium oxide nanoparticles as deposited from solution (dried in air at room temperature), and standard bulk cubic In_2O_3 reference spectrum (PDF no. 00−006−0416).

The transfer characteristics and output characteristics of a typical In_2O_3 nanocrystal TFT fabricated at the optimal conditions are shown in Figure 4, along with a schematic drawing of the device structure. Metal-oxide semiconductors are known to exhibit higher performance when they incorporate a gate dielectric material with a high dielectric

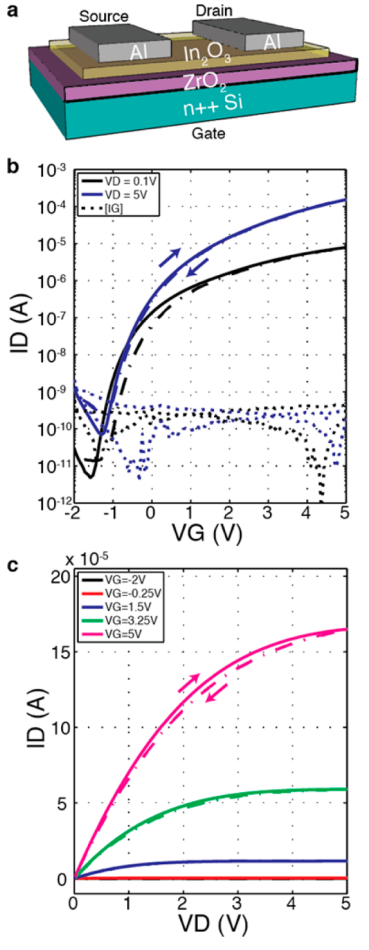

Figure 4. (a) Structure of the back-gate, top-contact In_2O_3 nanocrystal TFT. (b) Transfer characteristics and (c) output characteristics of a TFT utilizing the In_2O_3 nanocrystals from a typical synthesis (T_{Grow} = 250 °C following a vacuum degassing step) as the channel layer, after a 500 °C postdeposition anneal in oxygen.

DOI: 10.1021/acsami.5b00893
ACS Appl. Mater. Interfaces 2015, 7, 10069−10075

constant, particularly ZrO_2; thus, we employed a 41 nm layer of ZrO_2 deposited by ALD ($\kappa \approx 21$) and, as expected, the TFT performance exceeds the results shown in Figure 1 for the same nanocrystal synthesis protocol. This In_2O_3/high-κ device exhibits an electron mobility in the linear regime of 10.9 $cm^2/(V\ s)$, with an I_{ON}/I_{MIN} current ratio greater than 10^6 and turn-on voltage of −1.5 V. The minimal hysteresis, steep subthreshold swing of 0.3 V/decade, and good suppression of carriers in the off-state are evidence of a high quality semiconductor film with low trap density. Clear saturation is evident in the output characteristics, indicating good electrostatic control. These devices, to the best of our knowledge, exhibit a carrier mobility an order of magnitude higher than any previously reported In_2O_3 nanocrystal TFT,[25,26] and comparable to other solution-processed In_2O_3 TFTs.[13,14]

In this work, we show that In_2O_3 nanocrystal inks are a promising pathway toward high-performance, air-stable, solution-processed transistors. We have explored how In_2O_3 nanocrystal synthesis conditions impact TFT performance in the context of printed electronic devices. The ligands that are critical to controlling nanocrystal nucleation and growth also provide solubility and ink stability, but residual organic material in a TFT can degrade electronic performance. The nanocrystal TFTs in this work have undergone a postdeposition anneal to remove the surfactants from the nanocrystal surfaces, allowing the particles to form a high-quality semiconductor channel material. This in turn results in devices with excellent performance, significantly better than previous reports on indium oxide nanoparticle-based thin film transistors, and similar to results obtained using sol−gel inks. Given the ink stability benefits of nanoparticles, we thus posit that semiconductor nanocrystal inks are a promising route toward exploiting the physical properties or inorganic solids while leveraging the low-cost manufacturing methods of large-area printing. Continuing work is needed to reduce the temperature at which the ligands are removed, bringing down the total thermal budget for the device fabrication to potentially enable the use of plastic substrates and leverage low-cost roll-to-roll printing processes.

■ ASSOCIATED CONTENT

Supporting Information

Sensitivity of TFT performance to sol−gel sit time. Detailed experimental procedure for In_2O_3 nanocrystal synthesis and TFT fabrication. Impact of degassing on nanocrystal solubility. AFM measurement of In_2O_3 film thickness and surface roughness. The Supporting Information is available free of charge on the ACS Publications website at DOI: 10.1021/acsami.5b00893.

■ AUTHOR INFORMATION

Corresponding Authors

*E-mail: swisher@berkeley.edu.
*E-mail: viveks@eecs.berkeley.edu.

Author Contributions

S.L.S. designed the experiments with input from S.K.V. and V.S. S.L.S. synthesized and characterized the nanoparticles, fabricated and tested the TFTs, and analyzed the data. All authors discussed the results and commented on the manuscript.

Notes

The authors declare no competing financial interest.

■ ACKNOWLEDGMENTS

S.L.S. gratefully acknowledges support for this work from the National Science Foundation in the form of a Graduate Research Fellowship, and from the Intel Foundation for the Robert Noyce Memorial Fellowship in Microelectronics. Thanks to the Stacy Lab for use for the XRD, and to Dr. Jaewon Jang for collecting the XRD data. We acknowledge the UC Berkeley Marvell Nanolab and the Stanford Nanofabrication Facility for the necessary equipment and support to fabricate TFTs, and the Stanford Nanocharacterization Laboratory for use of the TEM.

■ ABBREVIATIONS

TFT, thin-film transistor
TEM, transmission electron microscopy
ALD, atomic layer deposition
XRD, X-ray diffraction
fwhm, full-width half-maximum
AFM, atomic force microscopy

■ REFERENCES

(1) Nathan, A.; Ahnood, A.; Cole, M. T.; Suzuki, Y.; Hiralal, P.; Bonaccorso, F.; Hasan, T.; Garcia-Gancedo, L.; Dyadyusha, A.; Haque, S.; Andrew, P.; Hofmann, S.; Moultrie, J.; Flewitt, A. J.; Ferrari, A. C.; Kelly, M. J.; Robertson, J.; Amaratunga, G. A. J.; Milne, W. I. Flexible Electronics: The Next Ubiquitous Platform. *Proc. IEEE* **2012**, *100*, 1486−1517.

(2) Sun, Y.; Rogers, J. A. Inorganic Semiconductors for Flexible Electronics. *Adv. Mater.* **2007**, *19*, 1897−1916.

(3) Kim, D.-H.; Ghaffari, R.; Lu, N.; Rogers, J. A. Flexible and Stretchable Electronics for Biointegrated Devices. *Annu. Rev. Biomed. Eng.* **2012**, *14*, 113−128.

(4) Subramanian, V.; Chang, J. B.; de la Fuente Vornbrock, A.; Huang, D. C.; Jagannathan, L.; Liao, F.; Mattis, B.; Molesa, S.; Redinger, D. R.; Soltman, D.; Volkman, S. K. Printed Electronics for Low-Cost Electronic Systems: Technology Status and Application Development. In *ESSCIRC 2008−34th European Solid-State Circuits Conference*; IEEE: Piscataway, NJ, 2008; pp 17−24.

(5) Street, R. A.; Wong, W. S.; Ready, S. E.; Chabinyc, M. L.; Arias, A. C.; Limb, S.; Salleo, A.; Lujan, R. Jet Printing Flexible Displays. *Mater. Today* **2006**, *9*, 32−37.

(6) Lee, K. H.; Park, J. H.; Yoo, Y. B.; Jang, W. S.; Oh, J. Y.; Chae, S. S.; Moon, K. J.; Myoung, J. M.; Baik, H. K. Effects of Solution Temperature on Solution-Processed High-Performance Metal Oxide Thin-Film Transistors. *ACS Appl. Mater. Interfaces* **2013**, *5*, 2585−2592.

(7) Jang, J.; Kitsomboonloha, R.; Swisher, S. L.; Park, E. S.; Kang, H.; Subramanian, V. Transparent High-Performance Thin Film Transistors from Solution-Processed SnO2/ZrO2 Gel-like Precursors. *Adv. Mater.* **2012**, *25*, 1042−1047.

(8) Street, R. A.; Ng, T. N.; Lujan, R. A.; Son, I.; Smith, M.; Kim, S.; Lee, T.; Moon, Y.; Cho, S. Sol-Gel Solution-Deposited InGaZnO Thin Film Transistors. *ACS Appl. Mater. Interfaces* **2014**, *6*, 4428−4437.

(9) Banger, K. K.; Yamashita, Y.; Mori, K.; Peterson, R. L.; Leedham, T.; Rickard, J.; Sirringhaus, H. Low-Temperature, High-Performance Solution-Processed Metal Oxide Thin-Film Transistors Formed by a "sol−gel on Chip" Process. *Nat. Mater.* **2011**, *10*, 45−50.

(10) Kim, M.-G.; Kanatzidis, M. G.; Facchetti, A.; Marks, T. J. Low-Temperature Fabrication of High-Performance Metal Oxide Thin-Film Electronics via Combustion Processing. *Nat. Mater.* **2011**, *10*, 382−388.

(11) Kim, H. S.; Byrne, P. D.; Facchetti, A.; Marks, T. J. High Performance Solution-Processed Indium Oxide Thin-Film Transistors. *J. Am. Chem. Soc.* **2008**, *130*, 12580−12581.

(12) Park, J. H.; Yoo, Y. B.; Lee, K. H.; Jang, W. S.; Oh, J. Y.; Chae, S. S.; Lee, H. W.; Han, S. W.; Baik, H. K. Boron-Doped Peroxo-

DOI: 10.1021/acsami.5b00893
ACS Appl. Mater. Interfaces 2015, 7, 10069−10075

Zirconium Oxide Dielectric for High-Performance, Low-Temperature, Solution-Processed Indium Oxide Thin-Film Transistor. *ACS Appl. Mater. Interfaces* **2013**, *5*, 8067−8075.
(13) Lee, J. S.; Kwack, Y.; Choi, W. Inkjet-Printed In(2)O(3) Thin-Film Transistor below 200 °C. *ACS Appl. Mater. Interfaces* **2013**, *5*, 11578−11583.
(14) Han, S.-Y.; Lee, D.-H.; Herman, G. S.; Chang, C.-H. Inkjet-Printed High Mobility Transparent−Oxide Semiconductors. *J. Display Technol.* **2009**, *5*, 520−524.
(15) Huang, D.; Liao, F.; Molesa, S.; Redinger, D.; Subramanian, V. Plastic-Compatible Low Resistance Printable Gold Nanoparticle Conductors for Flexible Electronics. *J. Electrochem. Soc.* **2003**, *150*, G412.
(16) Kovalenko, M. V.; Scheele, M.; Talapin, D. V. Colloidal Nanocrystals with Molecular Metal Chalcogenide Surface Ligands. *Science* **2009**, *324*, 1417−1420.
(17) Talapin, D. V.; Lee, J. S.; Kovalenko, M. V.; Shevchenko, E. V. Prospects of Colloidal Nanocrystals for Electronic and Optoelectronic Applications. *Chem. Rev.* **2009**, *110*, 389−458.
(18) Liu, Y.; Tolentino, J.; Gibbs, M.; Ihly, R.; Perkins, C. L.; Liu, Y.; Crawford, N.; Hemminger, J. C.; Law, M. PbSe Quantum Dot Field-Effect Transistors with Air-Stable Electron Mobilities above 7 cm2 V(−1) S(−1). *Nano Lett.* **2013**, *13*, 1578−1587.
(19) Nomura, K.; Ohta, H.; Takagi, A.; Kamiya, T.; Hirano, M.; Hosono, H. Room-Temperature Fabrication of Transparent Flexible Thin-Film Transistors Using Amorphous Oxide Semiconductors. *Nature* **2004**, *432*, 488−492.
(20) Hosono, H. Ionic Amorphous Oxide Semiconductors: Material Design, Carrier Transport, and Device Application. *J. Non. Cryst. Solids* **2006**, *352*, 851−858.
(21) Seo, W. S.; Jo, H. H.; Lee, K.; Park, J. T. Preparation and Optical Properties of Highly Crystalline, Colloidal, and Size-Controlled Indium Oxide Nanoparticles. *Adv. Mater.* **2003**, *15*, 795−797.
(22) Lee, C. H.; Kim, M.; Kim, T.; Kim, A.; Paek, J.; Lee, J. W.; Choi, S.-Y.; Kim, K.; Park, J.-B.; Lee, K. Ambient Pressure Syntheses of Size-Controlled Corundum-Type In2O3 Nanocubes. *J. Am. Chem. Soc.* **2006**, *128*, 9326−9327.
(23) Niederberger, M.; Garnweitner, G.; Buha, J.; Polleux, J.; Ba, J.; Pinna, N. Nonaqueous Synthesis of Metal Oxide nanoparticles:Review and Indium Oxide as Case Study for the Dependence of Particle Morphology on Precursors and Solvents. *J. Sol-Gel Sci. Technol.* **2006**, *40*, 259−266.
(24) Caruntu, D.; Yao, K.; Zhang, Z.; Austin, T.; Zhou, W.; O'Connor, C. J. One-Step Synthesis of Nearly Monodisperse, Variable-Shaped In 2 O 3 Nanocrystals in Long Chain Alcohol Solutions. *J. Phys. Chem. C* **2010**, *114*, 4875−4886.
(25) Cui, T.; Liu, Y.; Zhu, M. Field-Effect Transistors with Layer-by-Layer Self-Assembled Nanoparticle Thin Films as Channel and Gate Dielectric. *Appl. Phys. Lett.* **2005**, *87*, 183105.
(26) Dasgupta, S.; Kruk, R.; Mechau, N.; Hahn, H. Inkjet Printed, High Mobility Inorganic-Oxide Field Effect Transistors Processed at Room Temperature. *ACS Nano* **2011**, 9628−9638.
(27) Ridley, B. A.; Nivi, B.; Jacobson, J. M. All-Inorganic Field Effect Transistors Fabricated by Printing. *Science* **1999**, *286*, 746−749.
(28) Volkman, S. K.; Mattis, B. A.; Molesa, S. E.; Lee, J. B.; Vornbrock, A.; de la, F.; Bakhishev, T.; Subramanian, V. A Novel Transparent Air-Stable Printable N-Type Semiconductor Technology Using ZnO Nanoparticles. *IEEE Int. Electron Devices Meet.* **2004**, 769−772.
(29) Yin, Y.; Alivisatos, A. P. Colloidal Nanocrystal Synthesis and the Organic-Inorganic Interface. *Nature* **2005**, *437*, 664−670.
(30) Lu, X.; Tuan, H.-Y.; Korgel, B. a; Xia, Y. Facile Synthesis of Gold Nanoparticles with Narrow Size Distribution by Using AuCl or AuBr as the Precursor. *Chemistry* **2008**, *14*, 1584−1591.

DOI: 10.1021/acsami.5b00893
ACS Appl. Mater. Interfaces 2015, 7, 10069−10075